

PREPARATION OF TITANIUM MOLECULAR SPECIES SUPPORTED ON MESOSTRUCTURED SILICA BY DIFFERENT GRAFTING METHODS

G. Calleja*, R. van Grieken, R. García, J.A. Melero and J. Iglesias
Department of Experimental Sciences and Technology. ESCET. Rey Juan Carlos University,
28933, Móstoles (Madrid), Spain.

Keywords: Mesoporous, SBA-15, titanium, epoxidation, grafting

Published on:

Journal of Molecular Catalysis A: Chemical 182-183 (2002) 215-225

[doi:10.1016/S1381-1169\(01\)00468-X](https://doi.org/10.1016/S1381-1169(01)00468-X)

To whom the correspondence should be addressed. Phone: 34-91-4887006. Fax: 34-91-6647490.e-mail:
g.calleja@escet.urjc.es

Abstract

Titanium supported on SBA-15 mesoporous silica has been synthesised containing different titanium loadings prepared by chemical grafting using titanocene dichloride as precursor and over different treated silica surfaces. A comparative study using MCM-41 mesoporous silica as support is also reported. The type of silica support and its surface properties as well as the initial concentration of Ti precursor in the organic solution influences clearly the incorporation of Ti species. The materials after grafting treatment were characterized by different conventional techniques including XRD, FT-IR DR UV-Vis and nitrogen adsorption. The titanium containing SBA-15 silica shows hexagonal mesoscopic order and pore sizes up to 70 Å with surface areas up to 600 m²/g and titanium content ranging from 1 to 3 wt. %. DR UV-Vis of Ti containing SBA-15 silica after removal of the organic ligand shows the presence of Ti isolated species tetrahedrally coordinated and the absence of bulky TiO₂ phases. Likewise, these materials upon calcination were catalytically active for the epoxidation of styrene with TBHP exhibiting a significant selectivity toward the epoxide.

1. INTRODUCTION

Heterogenisation of catalytic homogeneous systems for selective oxidation reactions in liquid phase is currently showed as a priority research field. These heterogeneous systems display clear advantages compared to their homogenous counterparts such as ease of recovery and recycling of active species and consequently being more attractive from an environmental point of view. In this context, serious efforts have been addressed toward the preparation of heterogeneous Ti(IV) catalysts for oxidation reactions and numerous strategies have been described in the literature for the immobilisation of redox-active species within an inorganic matrix [1]. These methods include framework substitution, encapsulation of metal complexes and grafting or tethering of inorganic and organic metal precursors to the internal surface [2].

In this sense, framework substitution of Ti atoms in tetrahedral positions of molecular sieves (Ti-silicalite [3] and Ti-beta zeolites [4]) has received much attention in the past decade as the obtained materials have shown to be efficient selective oxidation catalysts [5]. However, their small pore size hinders the access of bulky substrates as well as of large organic hydroperoxides. To overcome this drawback, novel silica-based ordered mesoporous materials such as MCM-41 [6] and SBA-15 [7] are being widely used as inorganic supports of redox-active species. The narrow, controlled pore size distribution of these ordered hexagonal materials as well as their large pore openings and high surface area are attractive properties that make them useful as catalyst inorganic support materials [8-10].

First attempts to incorporate titanium species within these mesoporous materials were carried out by isomorphous substitution through hydrothermal crystallisation (Ti-MCM-41 [11], Ti-MCM-48 [12], Ti-HMS [13] and Ti-MSU [14]). However, the catalytic activity of

these modified mesoporous materials was quite small as compared to that shown by TS-1 and Ti-beta zeolites, probably because access by the reactants to active Ti centres might be limited as the Ti species are partially buried within the inner walls of the mesoporous materials. In order to overcome this drawback associated with hydrothermal crystallised Ti mesoporous materials, alternative approaches have been developed for the covalent attachment of Ti species onto the internal mesoporous silica surface. These methods are based on the grafting (directly) and tethering (with a spacer ligand) of a suitable inorganic and organometallic precursor by chemical reaction with the pendant silanol groups located on the surface of the mesopore walls. This method of preparation shows considerable advantages as compared to hydrothermal synthesis procedure because of the greater accessibility of the incorporated Ti centres to the reactants [15]. Among the different titanium precursors titanocene dichloride ((Cp₂)TiCl₂) is desirable as a grafting reagent in comparison to TiCl₄ and Ti(OR)₄ agents as either of the latter tend to the precipitation of anatase by-products during the grafting. Thomas et al. [16] grafted Ti(IV) species to the internal surface of MCM-41 by reaction with (Cp₂)TiCl₂ and subsequent calcination. Later, Corma et al. [17] following a procedure similar to that reported by Thomas et al. achieved the grafting of titanocene species on a silica named ITQ-2. These materials showed a better activity in epoxidation of olefins in presence of terbutylhydroperoxide (TBHP) than hydrothermally synthesised Ti-MCM-41 materials.

On the other hand, the incorporation of Ti species to silica-based SBA-15 materials through a direct synthesis procedure appears unlikely because the preparation needs a strong acidic media (2 M HCl). Necessarily, this incorporation might be achieved by “post-synthesis” grafting procedures involving reaction with a titanium precursor. Recently, Luan et al. [18] have synthesised Ti-SBA-15 via incipient-wetness impregnation with titanium isopropoxide in ethanol under inert atmosphere followed by calcination.

In this contribution, we have used $(\text{Cp}_2)\text{TiCl}_2$ as titanium precursor for the chemical grafting of Ti species onto the surface of ordered silica-based mesoporous SBA-15 materials through a similar procedure reported by Thomas et al. [16]. There is a considerable advantage of using $(\text{Cp})_2\text{TiCl}_2$ as Ti precursor because of its great stability in comparison with conventional titanium sources such as TiCl_4 and $\text{Ti}(\text{RO})_4$. Additionally, we have carried out a study of the influence of the silica surface properties on the incorporation degree of Ti species. The results obtained demonstrate that the incorporation of Ti species is strongly dependent on the concentration and nature of the silanol groups. Moreover, the Ti loading can be controlled modifying conveniently the surface properties of the raw materials.

2. EXPERIMENTAL SECTION

2.1 Samples preparation

2.1.1 Preparation of parent silica-based mesoporous materials. MCM-41 was synthesised according to the hydrothermal procedure described by Lin et al. [19] but using triethylamine (NEt_3 ; Acros) as mineralizing agent. Hexadecyltrimethyl ammonium chloride (Aldrich) was used as structure directing agent. It was dissolved in an aqueous solution of triethylamine at room temperature. After adding tetraethyl orthosilicate (TEOS, Alfa) the mixture was stirred for additional four hours and then charged into a teflon-line autoclave reactor followed by heating at 100°C for 48 hours. The resultant solid product was recovered by filtration, washed with distilled water and dried at room temperature. SBA-15 was prepared according to a procedure reported elsewhere by Zhao et al. [7] using Pluronic 123 triblock copolymer ($\text{EO}_{20}\text{-PO}_{70}\text{-EO}_{20}$; Aldrich) as polymeric template. In a typical synthesis: 4 g of Pluronic 123 was

dissolved under stirring in 125 g of 1.9 M HCl at room temperature. The solution was heated up to 40 °C before adding tetraethylorthosilicate (TEOS; Aldrich). The resultant solution was stirred for 20 h at 40 °C, followed by aging at 100 °C for 24 h under static conditions. The solid product was recovered by filtration and dried at room temperature overnight.

2.1.2 Surfactant removal procedures. The polymeric template was removed from as-made silica-based mesoporous materials through different techniques including thermal treatments and low-temperature solvent extraction. Thus, according to the thermal treatment, the as-synthesized silica MCM-41 and SBA-15 materials were calcined for 7 hours at 550 °C in air atmosphere. These materials are denoted as MCM-*c* and SBA-*c*, respectively. Alternatively, following the method reported by Zhao et al. [7], block copolymer was removed from as-made SBA-15 materials by washing with ethanol under reflux in a magnetically stirred flask for 24 hours (1.5 g. of as-synthesized material per 400 ml. of ethanol). On the other hand, the removal of surfactant in the synthesized MCM-41 material was achieved using acidified ethanol under reflux [20] (1.5 g of as-synthesized as-made MCM-41 was refluxed for 24 h. in 210 g of 1.5 wt. % HCl/ 2.5 % wt. H₂O/ethanol mixture). The extracted materials are denoted as MCM-*e* and SBA-*e*.

2.1.3 Silylation procedure. The surface of the calcined silica-based materials was end-capped with trimethylchlorosilane (TMCS; Aldrich) through a grafting procedure. In a typical preparation, an appropriate amount of TMCS was dissolved in 90 g. of chloroform followed by addition of the outgassed silica material (TMCS/ raw material mass ratio of 0.6). The resultant solution was kept under stirring at room temperature during 1 hour. The final silylated product was recovered by filtration and intensively washed with chloroform. The silylated materials are denoted as MCM-*s* and SBA-*s*.

2.1.4 *Grafting procedure.* Titanium grafted onto the MCM-41 and SBA-15 surface was achieved starting from calcined (*c*), extracted (*e*) and silylated (*s*) materials according to the grafting technique proposed by Thomas and co-workers [16] using a solution of titanocene dichloride ($(\text{Cp}_2)\text{TiCl}_2$; Acros). Materials, prior to the grafting, were outgassed under vacuum conditions overnight. The sample was then stirred in a solution of $(\text{Cp}_2)\text{TiCl}_2$ in 90 g of chloroform under a dry nitrogen atmosphere for 1 hour. Thereafter, triethylamine ($\text{NEt}_3/(\text{Cp}_2)\text{TiCl}_2$ molar ratio of 1) was added to the suspension to promote surface silanols activation [21]. The resultant solution was kept under stirring for additional 2 hours. Finally, the solids were recovered by filtration and intensively washed with chloroform. Different loading of titanium were tested with mass ratios of $(\text{Cp}_2)\text{TiCl}_2$ to raw material in the organic solution ranging from 0.4 to 0.1.

2.2 Samples characterisation

X-ray powder diffraction (XRD) data were acquired on a PHILIPS diffractometer using $\text{Cu K}\alpha$ radiation. Typically, the data were collected from 0.6 to 4° (2θ) with a resolution of 0.02° . Fourier transform IR (FT-IR) spectra were recorded by means of a MATTSON spectrophotometer using the KBr wafer technique. For each sample, 128 IR spectra were added to achieve acceptable signal to noise levels. Diffuse reflectance UV-VIS spectra (DR UV-VIS) were obtained under ambient conditions on a CARY-1 spectrophotometer equipped with a diffuse reflectance accessory in the wavelength range of 200- 600 nm.

Nitrogen adsorption-desorption isotherms at 77 K were determined using an adsorption porosimeter (Micromeritics, TRISTAR 3000). The surface area measurements were

performed according to the BET method. Pore size distribution was obtained applying the BJH model with cylindrical geometry of the pores and using the Harkins and Jura equation for determining the adsorbed layer thickness. The pore volume was taken at $P/P_0 = 0.985$ single point.

The organic content was determined using a CHNS analyser (LECO, 932 model), and the titanium content was determined by ICP-atomic emission spectroscopy. The samples (100 mg) were dissolved in aqueous hydrofluoric acid. After dissolution, the sample was transferred into 1 L calibrated flask and diluted with water. An absorption standard solution of Ti ($1000 \mu\text{g mL}^{-1}$ in water) was used for the calibration of the equipment.

Catalytic tests of styrene epoxidation were carried out in a batch reactor equipped with a temperature controller and pressure gauge at 60°C for 1 hour under stirring. All the reactants and the catalyst were charged into the teflon-lined reactor and the system was heated up to 60°C . *Tert*-butyl hydroperoxide (TBHP; 70 wt % aqueous solution; Aldrich) was used as oxidant and acetonitrile (ACN; Scharlab) as solvent (TBHP /styrene molar ratio= 0.4, ACN/styrene mass ratio=5, styrene/catalyst mass ratio= 30 and catalyst=0.1 g). The stability of the catalysts was analyzed as follows: solid was recovered from the solution by filtration after the reaction, calcined at 550°C for 5 h in order to remove any organic species remaining adsorbed and finally tested again at the same reaction conditions. This procedure was repeated twice. All the reaction products were analysed by gas chromatography (VARIAN 3380) on a capillary column DB-6.

3. RESULTS AND DISCUSSION

3.1 Characterisation of the samples

Table 1 lists the Ti containing materials prepared under different conditions and their titanium contents. The incorporation of titanium species over calcined SBA-15 samples is lower than that expected based on the titanium loading of the initial solution. Likewise, the incorporation degree decreases gradually as the Ti content increases in the initial organic solution. A similar trend is observed when calcined MCM-41 samples are used as raw materials, although in this particular case the maximum percentage of Ti grafted on the silica surface starting from organic solutions with similar content in $(\text{Cp}_2)\text{TiCl}_2$ is significantly lower than that measured in Ti-SBA-15 materials (2.0% vs. 3.0%). The surface properties of the silica support should influence significantly on the incorporation degree of Ti species. In this way, extracted silica based materials with a high concentration of silanols groups, not thermally reacted by condensation, should achieve a more efficient incorporation of titanium species. The figures in Table 1 (samples 13-16) show that this effect is almost negligible for SBA-15 materials although an increase of the incorporation is readily evidenced for extracted MCM-41 materials. These results suggest that the reactive nature of silanol groups for both materials is significantly different. Moreover, when the amount of hydroxyl groups located on the surface are diminished by silylation reaction with methyl groups, the anchoring of Ti species is dramatically depressed. The results clearly show that the anchoring of Ti species on the surface of mesoporous materials is undoubtedly imposed not only by the concentration of the Ti precursor in the organic solution, but also by the type of material and its surface properties.

Table 2 shows the C/Ti molar ratio of calcined SBA-15 materials after grafting of different concentrations of $(Cp_2)TiCl_2$. Thomas et al. [16] concluded, according to their EXAFS and FTIR experiments over MCM-41 supporting $(Cp_2)TiCl_2$ species, that the Ti^{+4} ion is anchored via three oxygens (each one linked to a silicon atom) and coordinated to one *cp* ring. This observation is in agreement with the expected trend of Ti species to be anchored through three bonds to the support which leads to the loss of a *cp* ligand as it was suggested by Thomas et al. [16]. Assuming that, the molar ratio of C/Ti of the samples synthesised in this work should be 5. However, our analytical results show a higher value of the C/Ti molar ratio for both SBA-15 and MCM-41 type materials, which decreases gradually with the amount of Ti species anchored on the silica surface. This C/Ti decrease, which is more pronounced in MCM-41 materials, might be attributed to the increasing of steric constraints imposed by the gradual lowering of pore size with the extent of Ti incorporation. It must be also noticed, that the above mentioned work [16] was carried out for samples with a Ti content of 6.76 wt. %, much higher than those achieved in the present work (maximum percentage of ca. 3 %). The experimental data showed here suggest that an increase of Ti incorporation induce significant changes on the coordination number of the Ti atoms. Furthermore, a relative low Ti loading supported on the mesoscopic silica surface allows the presence of two *cp* ligands attached to the Ti atom. The use of SBA-15 instead of MCM-41 allows to keep the C/Ti ratio close to that present in the $(Cp)_2TiCl_2$ for Ti loadings up to 3.0%, probably due to the higher pore size, which avoids the loss of one *cp* ligand of the anchored complex. The wider pores present in the SBA-15 material probably induces less interaction of the silanol groups with the titanium complex, preventing further reaction once it is anchored on the silica surface. Another possible contribution for explaining the differences observed in the chemical composition of the complex anchored on the silica surface when MCM-41 and SBA-15 materials are used as support, is related with the different chemical reactivity of the

silanol groups, a feature that has been shown when calcined and extracted mesoporous materials are compared in terms of anchoring efficiency of the $(\text{Cp})_2\text{TiCl}_2$ compound.

Low-angle XRD patterns of siliceous calcined SBA-15 and Ti –SBA-15 with different Ti loading (samples 5-8; Table 1) are depicted in Figure 1 (a). A well-resolved pattern with a significant peak at ca. 0.8° and two smaller at ca. 1.6° and ca. 1.7° are clearly evidenced for all the samples indicating a good mesoscopic order. It can be seen that grafting of Ti species influences on the unit cell parameter, as evidenced by the decreasing of the d_{100} spacings for the titanium modified materials. Figure 1(b) show low-angle XRD spectra for Ti-SBA-15 materials obtained from grafting over extracted SBA-15 mesoporous materials (samples 13-16; Table 1). The observed peaks for the titanium modified materials show a gradual change in the d_{100} spacing with the increasing of titanium content.

Figure 2 (a) shows nitrogen adsorption/desorption isotherms from calcined SBA-15 and the corresponding grafted materials with different loading of Ti. All the materials give typical type IV adsorption isotherms with a H1 hysteresis loop [22]. The calculated BET area for the calcined parent material is around $600 \text{ m}^2/\text{g}$ and decreases with increasing titanium loading (Table 3). The isotherm of the calcined parent SBA-15 material exhibits a sharp inflection at $P/P_0=0.7$ characteristic of capillary condensation within the uniform pores (Figure 2 (a)). As the amount of Ti species increases, Ti-SBA-15 materials show isotherms with similar inflection but with reduced sharpness and at lower P/P_0 . When this comparison is made for extracted SBA-15 parent materials anchored with different Ti loading contents a similar trend is observed (not shown).

Pore size distribution of the different mesoporous materials have been determined using the BJH model widely used for this type of samples [23]. Although this model systematically underestimates pore sizes [24], it is appropriate for comparative purposes in this work, since we are interested in changes occurring in the pore size after grafting treatment and not in the absolute values. Average BJH values of the pore diameter are given in Table 3 showing a gradual decrease with the incorporation degree of Ti species. Pore size distribution of the different samples using the BJH model is depicted in Figure 2 (b). Average pore diameter clearly diminishes with the incorporation of Ti species, which is attributed to the internal lining of mesopores with TiCp_2 functionalities thus reducing the pore diameter and increasing the wall thickness. In this way, the sample with the highest amount of Ti species (samples 7 and 8; Table 3) exhibits a significant decrease in the surface area and pore volume, as well as an increase in the wall thickness measured through the difference between the interplanar spacing d_{100} , and the pore size determined by BJH model. However, the very narrow pore size distribution for all the cases is a strong indication of the homogeneous dispersion of Ti species onto the silica surface.

FT-IR spectra of the different materials are depicted in Figure 3. A weak vibration centred at 1400 cm^{-1} corresponding to the stretching vibration of the C=C bond is clearly visible for the cyclopentadienyl titanium-grafted material (sample *b*; Figure 3). On the other hand, this signal is absent in the parent SBA-15 material (sample *a*; Figure 3) and in the grafted material after calcination (sample *d*, Figure 3). Therefore, this signal reveals the presence of cyclopentadienyl (*cp*) groups on the surface of the silica support. Additionally, the band at 960 cm^{-1} is conventionally a fingerprint of the existence of Si-O-Ti bonds in zeolites and its increase correlates with the incorporation of Ti into the framework [25]. However, as it can be seen in Figure 3, this band also appears in the spectra of Ti-free SBA-15

material (sample a; Figure 3). FT-IR studies carried out by Blasco et al. in mesoporous materials demonstrate that this vibration should be assigned to the abundance of silanol groups [26]. As a consequence of the above-mentioned fact, this band cannot be used as an absolute criterion to claim the presence of titanium in the framework in this kind of materials. Finally, the silylated titanium-modified materials exhibit a clear signal at 2900 cm^{-1} which indicates the presence of methyl groups attached to the silica surface (sample c; Figure 3) accompanied with a significant decrease of the broad signal corresponding to the silanol groups (centred at 3500 cm^{-1}).

Figure 4 shows DR-UV VIS spectra of different series of Ti-SBA-15 materials. This spectroscopic technique has been commonly used for the assessment of Ti atoms environment in silica based materials [27]. The UV-Vis spectra of the cyclopentadienyl titanium-grafted materials (sample 5-8; Table 1) exhibit three different signals: an absorption band centred at 215 nm, a band at 255 nm and a broad signal at 350 nm. The latter signals increase clearly with the incorporation of Cp_2Ti species on the silica surface of the mesoporous materials. The band at ca. 220 nm in Ti-substituted mesoporous materials have been assigned to isolated Ti(IV) framework sites similar to those found in TS-1 materials [28-29]. These studies also report that a broad absorption band centred at 330 nm is a strong indication of bulk titania phases [27]. Calcination of the samples under air atmosphere removes entirely the *cp* ligands and the resulting materials display a unique signal centred at 220 nm (Figure 3, right top, sample e) without evidence of titania phases. This fact suggests that signals observed at 255 and 350 nm are attributed to the presence of organic *cp* species. Moreover, the spectrum of the Ti modified SBA-15 material free of *cp* ligands is quite similar to that corresponding to a zeolitic TS-1 material (Figure 3, right top, sample f). Nevertheless, a slight shoulder is evidenced for the Ti mesoporous material arising from partially polymerised hexacoordinated

titanium species or very small titania nanodomains [27]. These spectroscopic results confirm good titanium dispersion on the silica surface of titanocene grafted materials upon calcination and free of bulk titania phases. Likewise, DR UV-Vis spectra of effectively anchored titanocene species are considerably different to those obtained for the titanocene dichloride precursor (Figure 3, right bottom, sample *g*).

3.2 Catalytic experiments

Catalytic performance of the Ti substituted SBA-15 materials has been tested in the epoxidation of styrene at 60 °C in presence of TBHP as oxidant agent and acetonitrile as solvent. A titanocene-grafted material (sample 5; Table 1) and a Ti-SBA-15 material free of organic *cp* ligands (sample 5 after calcination) have been checked. For comparison, a homogeneous catalytic run carried out with dissolved $(Cp)_2TiCl_2$ has been also tested under modified reaction conditions related to the titanium concentration, six times higher than that corresponding to heterogeneous catalytic reactions. The epoxidation of styrene over the different catalytic systems yields mainly three kinds of products: epoxide, phenylalcaldehyde (epoxide isomerization) and benzaldehyde (oxidative epoxide cleavage). Table 4 lists the epoxide conversion and the selectivity towards reaction products as well as the turnover number, which allows a comparative study of the catalytic performance of the different catalysts.

First of all, epoxidation catalytic tests were carried out in presence of a Ti-free SBA-15 material (run 1; Table 4). The catalytic results show that the supported-catalysed contribution to the styrene epoxidation is low (styrene conversion of ca. 4.1%) and

consequently the activity of the different materials must be attributed to presence of active Ti centres.

The presence of *cp* ligands has a significant influence on the styrene conversion and products selectivity. Titanocene-grafted material (run 2, Table 4) exhibited a high substrate conversion but a relative low epoxide selectivity and a significant formation of bulky compounds arising from olefin polymerization. These results would be fairly in agreement with works described in the literature dealing with the efficiency of metal cyclopentadienyl species for the polymerization processes [30]. However, the titanocene material upon calcination displays a higher selectivity toward the epoxide formation with negligible formation of bulky compounds. Likewise, the turnover number of this material is comparable to that reported for Ti-MCM-41 [16] although both catalysts have been tested with different substrates. Finally, the activity of the Ti-SBA-15 material has been compared with a catalytic homogeneous system consisting of dissolved titanocene dichloride. The results show that Ti species anchored to the surface of mesopore walls produce a higher activity than those directly dissolved in the reaction medium.

Another important issue of the catalytic performance of this type of catalysts is their stability towards Ti leaching. In order to study this effect, Ti-SBA-15 material free of *cp* ligands was recycled twice, being the results showed in Figure 5. The conversion and product distribution obtained were practically constant, thus indicating a good stability of this catalyst.

4. CONCLUSIONS

Titanium containing mesoporous silica SBA-15 has been synthesised using titanocene dichloride as metallic precursor. In contrast with the work published by Thomas et al. [16], where just one *cp* ligand remains attached to the Ti centre after grafting treatment (C/Ti coordination number of 5), our results show that a significant amount of Ti species remain linked to both *cp* ligands after grafting treatment. Moreover, the C/Ti coordination number is dramatically influenced by the amount of Ti effectively anchored on the surface. The presence of two free covalent positions of a Ti atom anchored to the surface of pore wall opens up the feasibility of new subsequent modifications for the covalent attachment of different organic functionalities.

The surface properties of the silica support are crucial for the incorporation degree of titanium species via titanocene dichloride. Adsorption and spectroscopic results reveal that the titanium is well dispersed on the silica surface and free of bulky titania phases. These titanocene grafted SBA-15 materials upon calcination are efficient catalysts for epoxidation reactions and show a high selectivity towards the epoxide formation.

Additionally, the work reported here is one more contribution of using $(Cp_2)TiCl_2$ for the anchoring of titanium species onto the surface of mesostructured silica pore walls.

5. ACKNOWLEDGEMENTS

This research was supported by the fund provided by the regional government of Madrid (Dirección General de Investigación: Contrato Programa – Grupo estratégico de URJC).b

5. REFERENCES

- [1] R.A. Sheldon, I.W.C.E. Arends, H.E.B. Lempers, *Catal. Today* 41 (1998) 387
- [2] I.W.C.E. Arends, R.A. Sheldon, *Appl. Catal. A*, 212 (2001), 175-187.
- [3] M. Tamarasso, C.Perego, B. Notari, *US Pat.*, 4 410 501, 1983.
- [4] M.A. Camblor, A. Corma, A. Martínez and J. Pérez-Pariente, *J. Chem. Soc., Chem. Commun.* (1992) 589.
- [5] G. Bellussi, M.S. Rigutto, *Advanced Zeolite Science and Application*. Elsevier Sci. Publishers B.V., Amsterdam, 1994.
- [6] C.T. Kresge, M.E. Leonowicz, W.J. Roth, J.C. Vartuli, J.S. Beck, *Nature* 359 (1992) 710.
- [7] D. Zhao, J. Feng, Q. Huo, N. Melosh, G.H. Fredrickson, B.F. Chmelka, G.D. Stucky, *Science* 279 (1998) 548.
- [8] K.Moller, T.Bein, *Chem. Mater.* 10 (1998) 2950.
- [9] J.H. Clark, D.J. Macquarrie, *J. Chem. Soc., Chem. Commun.* (1998) 853.
- [10] A. Tuel, *Microporous&Mesoporous Mater.* 27 (1999) 151.
- [11] A. Corma, M.T. Navarro, J. Pérez-Pariente, *J. Chem. Soc., Chem. Commun.* (1994) 147.
- [12] M. Morey, A. Davidson, G. Stucky, *Microporous Mater.* 6 (1996) 99.
- [13] P.T.Tanev, M. Chibwe, T.J. Pinnavaia, *Nature* 368 (1994) 321.
- [14] S.A. Bagshaw, E. Pouzet, T.J. Pinnavaia, *Science*, 296 (1995) 1242.
- [15] R.D: Oldroyd, J.M. Thomas, T. Maschmeyer, P.A. MacFaul, D.W. Snelgrove, K.U. Ingold, D.D. M. Wayner, *Angew. Chem., Int. Ed. Engl.* 35 (1996) 2787.
- [16] T. Maschmeyer, F. Rey, G. Sankar, J. M. Thomas, *Nature* 378 (1995) 159-162.
- [17] A. Corma, U. Diaz, V. Fornés, J.L. Jordá, M. Domine, F. Rey, *J. Chem. Soc, Chem. Commun.* (1999) 779.

- [18] Z. Luan, E.M. Maes, P.A. W. van der Heide, D. Zhao, R.S. Czernuszewicz, L. Kevan, *Chem. Mater.* 11 (1999) 3680.
- [19] W. Lin, Q. Cai, W. Pang, Y. Yue, B. Zou, *Microporous&Mesoporous Mater.* 33 (1999) 187.
- [20] K. Moller, T. Bein, R.X. Fischer, *Chem. Mater.* 11 (1999) 665-673.
- [21] N.R.E.N. Impens, P. van der Voort, E.F. Vansant, *Microporous&Mesoporous Mater.* 28 (1999) 217.
- [22] K.S. W. Sing, D.H. Everett, R.A.W. Haul, L. Moscow, R.A. Pierotti, J. Rouquerol, T. Siemieniewska, *Pure Appl. Chem.* 57 (1985) 603.
- [23] P.T. Tanev, L.T. Vlaev, *J. Colloid Interface Sci.* 160 (1993) 110.
- [24] W.W. Jr Lukens, P. Schmidt-Winkel, D. Zhao, J. Feng, G.D. Stucky, *Langmuir*, 15 (1999) 5403.
- [25] M.R. Boccuti, K.M. Rao, A. Zecchina, G. Leofanti, G. Petrini, *Stud. Surf. Sci. Catal.* 48 (1989) 133.
- [26] T. Blasco, A. Corma, M.T. Navarro, J.P. Pariente, *J. Catal.* 156 (1994) 65.
- [27] F. Geobaldo, S. Bordiga, A. Zecchina, E. Gianello, G. Leofanti and G. Petrini, *Catal. Lett.*, 16 (1992) 109.
- [28] W. Zhang, J. Wang, P.T. Tanev, T.J. Pinnavaia, *J. Chem. Soc. , Chem Commun.* (1996) 976.
- [29] W. Zhang, M. Froba, J. Wang, P.T. Tanev, J. Wong, T.J. Pinnavaia, *J. Am. Chem. Soc.* 118 (1996) 9164.
- [30] L. Resconi, L. Cavallo, A. Fait, F. Piemontesi, *Chem. Rev.* 100 (2000) 1253.

Table 1. Efficiency of grafting procedure for the different silica-based materials.

Sample	Material	Ti content		Inc. (%)	Sample	Material	Ti content		Inc. (%)	Sample	Material	Ti content		Inc. (%)
		Ti ^T (%) ^a	Ti ^C (%) ^b				Ti ^T (%) ^a	Ti ^C (%) ^b				Ti ^T (%) ^a	Ti ^C (%) ^b	
1	MCM- <i>c</i>	2.0	1.1	55.0	9	MCM- <i>e</i>	2.0	1.2	60.0	17	MCM- <i>s</i>	2.0	0.4	20.0
2	MCM- <i>c</i>	4.0	1.4	35.0	10	MCM- <i>e</i>	4.0	2.0	50.0	18	MCM- <i>s</i>	4.0	0.4	10.0
3	MCM- <i>c</i>	6.0	2.1	35.0	11	MCM- <i>e</i>	6.0	3.3	55.0	19	MCM- <i>s</i>	6.0	0.7	11.2
4	MCM- <i>c</i>	8.0	2.1	26.3	12	MCM- <i>e</i>	8.0	3.5	43.8					
5	SBA- <i>c</i>	2.0	1.2	60.0	13	SBA- <i>e</i>	2.0	1.3	65.0	20	SBA- <i>s</i>	2.0	1.0	50.0
6	SBA- <i>c</i>	4.0	1.6	40.0	14	SBA- <i>e</i>	4.0	1.5	38.0	21	SBA- <i>s</i>	4.0	1.1	27.5
7	SBA- <i>c</i>	6.0	3.0	50.0	15	SBA- <i>e</i>	6.0	2.2	36.7	22	SBA- <i>s</i>	6.0	1.2	20.0
8	SBA- <i>c</i>	8.0	2.9	36.2	16	SBA- <i>e</i>	8.0	2.5	31.2					

^a Maximum Ti loading ^b Mass composition measured by I.C.P.

Table 2. C/Ti molar ratio for the different calcined silica-based materials after grafting treatment

Sample	Material	C/Ti ^a	Sample	Material	C/Ti ^a
1	MCM- <i>c</i>	9.1	5	SBA- <i>c</i>	10.0
2	MCM- <i>c</i>	8.7	6	SBA- <i>c</i>	10.0
3	MCM- <i>c</i>	7.2	7	SBA- <i>c</i>	9.5
4	MCM- <i>c</i>	6.6	8	SBA- <i>c</i>	8.9

^a Molar ratio of C/Ti in the grafted materials

Table 3. Textural properties of different Ti substituted SBA-15 materials.

Sample	Pore diameter (Å)	Surface Area (m ² /g)	Pore Volume (cm ³ /g)	d ₍₁₀₀₎ (Å)	Wall thickness (Å)
Calcined Support	73	605	0.92	88	30
5	74	502	0.82	94	34
7	68	438	0.69	94	40
8	67	455	0.69	92	39

Table 4. Catalytic results of different Ti substituted SBA-15 materials in the epoxidation of styrene with TBHP in liquid phase.

Run	Catalyst	TOF (mol/mol Ti·min)	Styrene conversion (%)	Selectivity towards reaction products			
				Styrene Oxide	Benzaldehyde	Phenyl Acetaldehyde	Others ^b
1	Blank ^a	-	4.1	56.7	37.8	5.5	0
2	Sample 5	5.8	23.8	35.2	7.4	2.7	54.8
3	Sample 5 upon calcination	2.3	9.9	76.0	16.3	7.7	0
4	Cp ₂ TiCl ₂ (Homogeneous)	0.6	10.7	65.0	30.0	5.0	0

^a Calcined silica based SBA-15 free of Ti atoms. ^b Bulky products arising from styrene oxide polymerisation.

Figure captions

Figure 1. XRD spectra of titanium substituted SBA-15 materials **(a)** Samples with different titanium loading over calcined SBA-15 material (a) Ti-free SBA-15, (b) Sample 5, (c) Sample 6, (d) Sample 7 and (e) Sample 8 **(b)** Samples with different Ti loadings over extracted SBA-15 material (a) Ti-free SBA-15, (b) Sample 13, (c) Sample 14, (d) Sample 15 and (e) Sample 16.

Figure 2. **(a)** N₂ adsorption / desorption isotherms of Ti substituted SBA-15 materials and **(b)** pore size distributions: (a) Calcined Ti-free SBA-15, (b) Sample 5, (c) Sample 7 and (d) Sample 8 .

Figure 3. FT- IR spectra of (a) Calcined SBA-15 material free of Ti species, (b) Cyclopentadienyl titanium anchored on a calcined SBA-15 material, sample 6, (c) Cyclopentadienyl titanium anchored on a silylated SBA-15 material, sample 20 and (d) Sample 6 upon calcination.

Figure 4. DR UV-Vis spectra of titanium grafted SBA-15 materials. (a) Sample 5, (b) Sample 6 , (c) Sample 7, (d) Sample 8, (e) Sample b after calcination (f) TS-1 zeolite and (g) Titanocene dichloride precursor.

Figure 5. Stability of Ti substituted SBA-15 catalyst in the styrene epoxidation with TBHP in liquid phase.

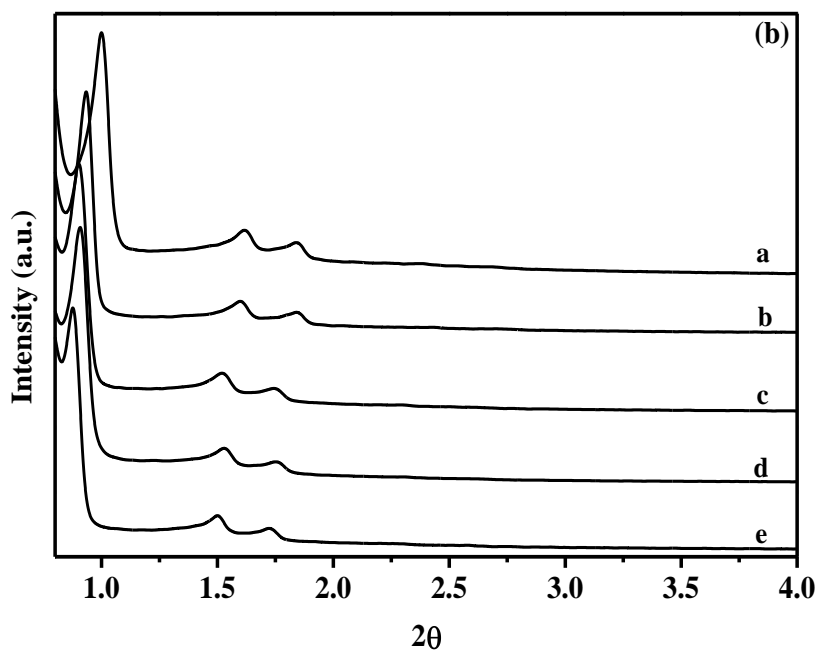
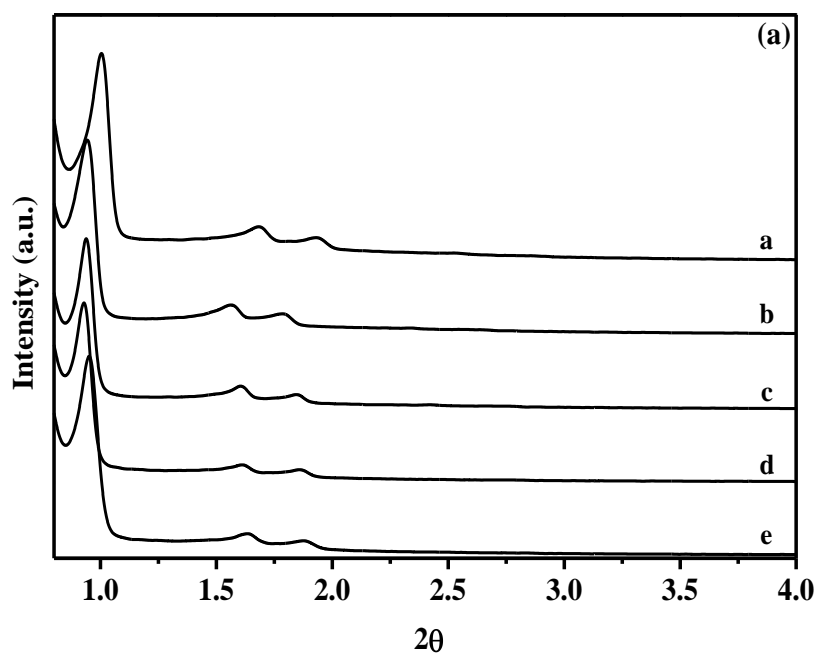


Figure 1.
Preparation of titanium molecular species supported on
G. Calleja et al.

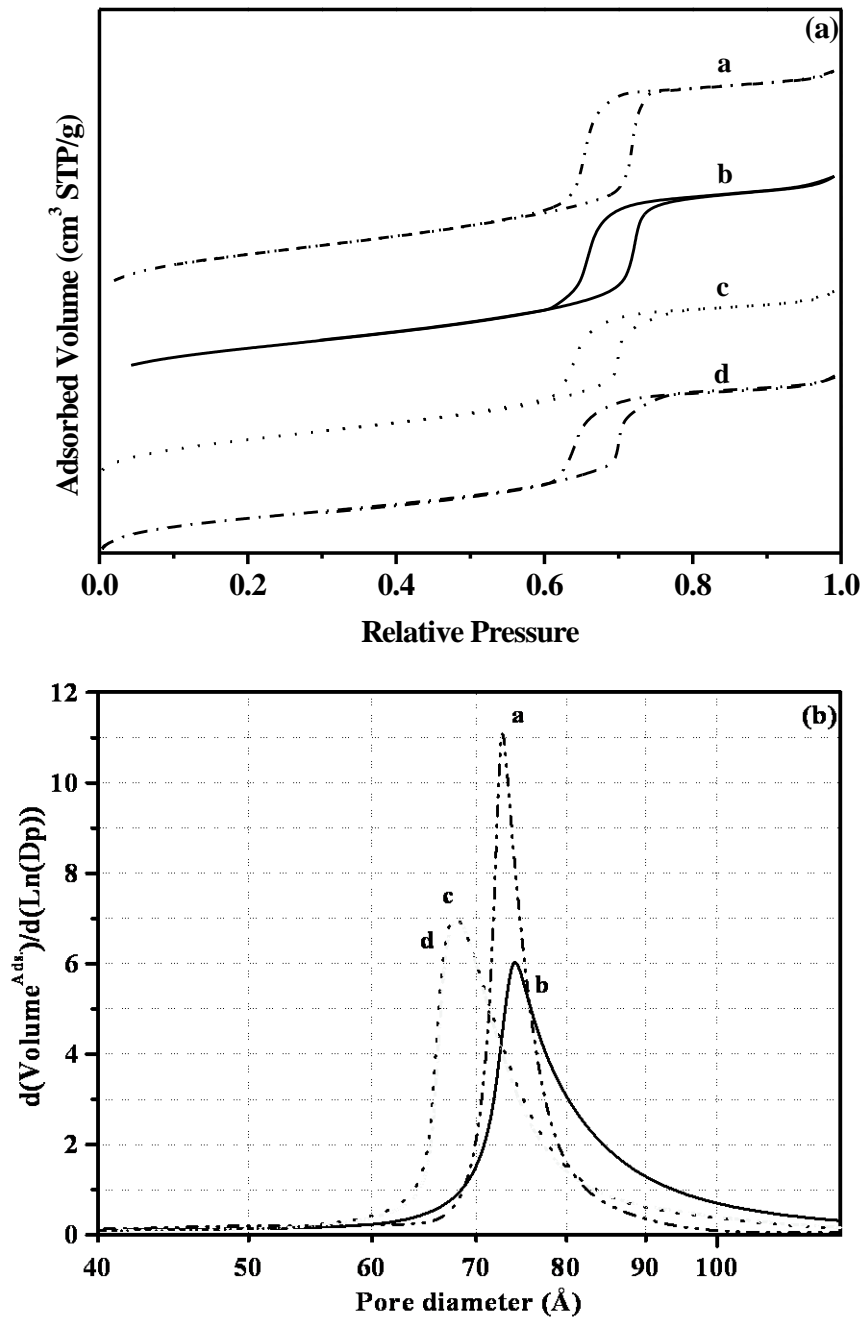


Figure 2.
Preparation of titanium molecular species supported on
G. Calleja et al.

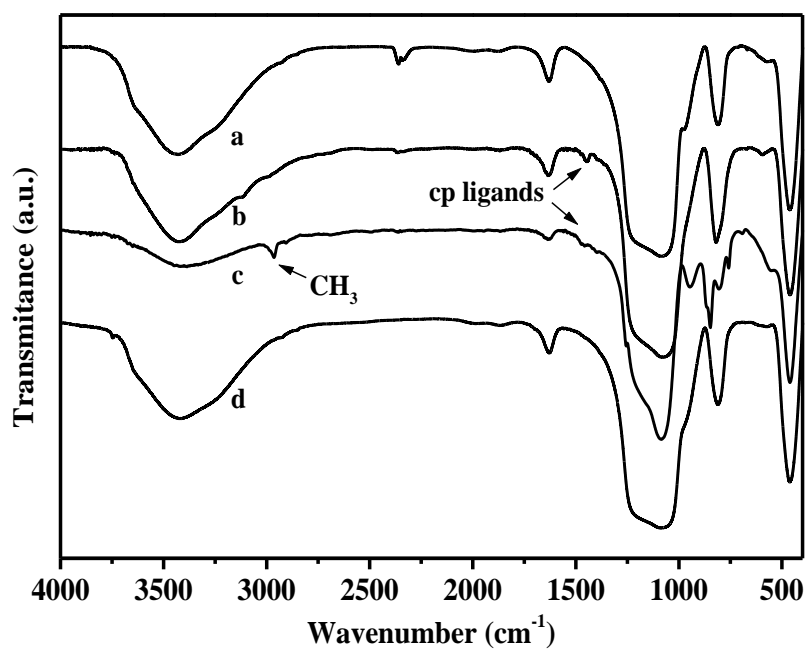


Figure 3.
Preparation of titanium molecular species supported on
G. Calleja et al.

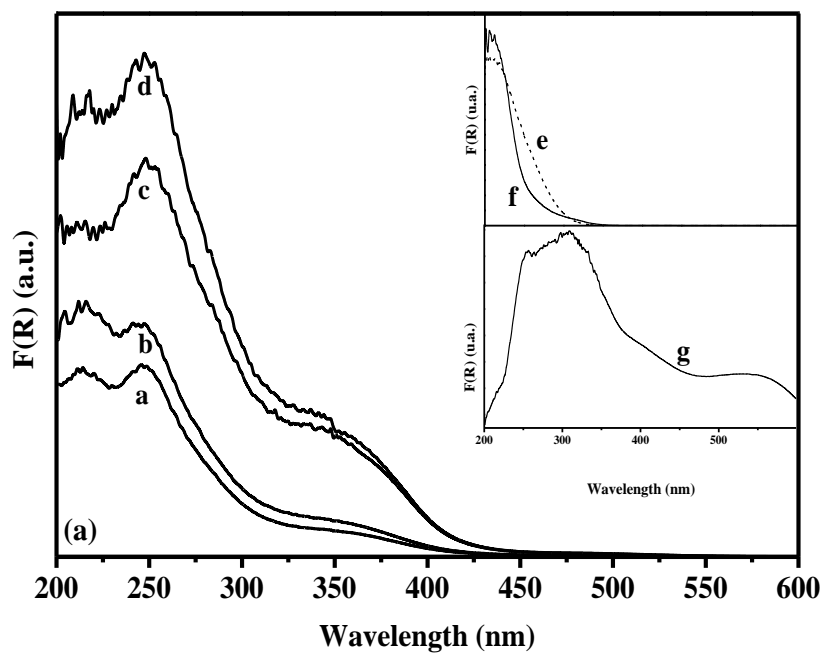


Figure 4.
Preparation of titanium molecular species supported on
G. Calleja et al.

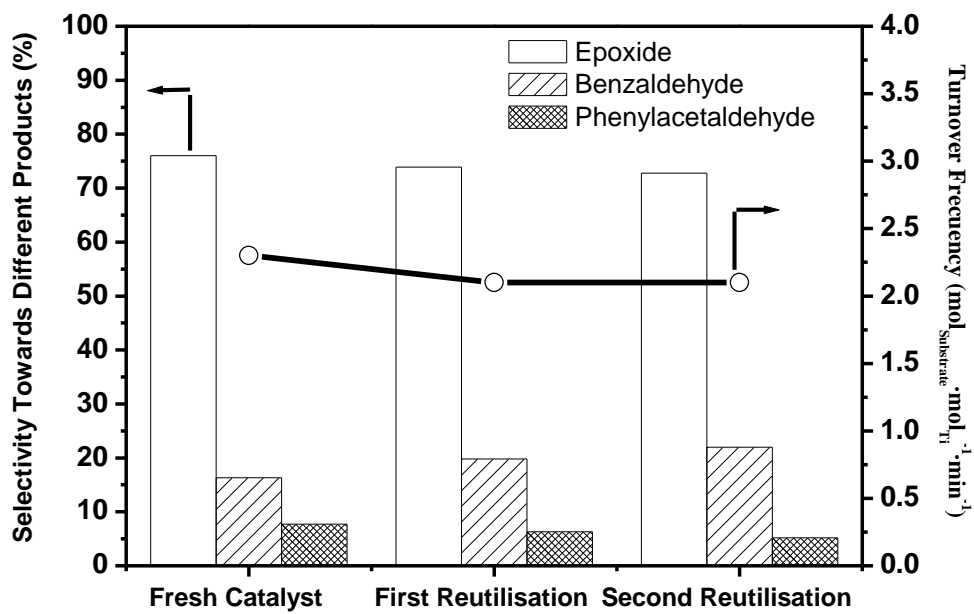


Figure 5.
Preparation of titanium molecular species supported on
G. Calleja et al.